

Evaluation of the precipitation of the East Asia regional reanalysis system mainly over mainland China

Linyun Yang  | Xudong Liang | Jinfang Yin | Yanxin Xie | Huiyi Fan

State Key Laboratory of Severe Weather,
The Chinese Academy of Meteorological
Sciences, Beijing, China

Correspondence

Xudong Liang and Jinfang Yin, State Key Laboratory of Severe Weather, The Chinese Academy of Meteorological Sciences, Beijing, China.
 Email: liangxd@cma.gov.cn (X. L.) and
 Email: yinjf@cma.gov.cn (J. Y.)

Funding information

The Basic Research Fund of Chinese Academy of Meteorological Sciences, Grant/Award Number: 2021Y030; The Joint Funds of the National Natural Science Foundation of China, Grant/Award Number: U2142214; The National Key R&D Program of China, Grant/Award Number: 2021YFC3000904; The National Key Research and Development Program of China, Grant/Award Number: 2017YFC1501800

Abstract

In this article, precipitation in a new regional reanalysis dataset, namely, the East Asia regional reanalysis system (EARS-CMA) with a 12-km resolution based on the Weather Research and Forecast (WRF) model, ERA-Interim, ERA5, TRMM 3B42V7, Climate Prediction Center Morphing Technique (CMORPH) and CN05.1, is compared in 2008–2017. The results show that EARS-CMA can capture the spatial features and temporal variation in precipitation over East Asia well. Focusing on mainland China, CMORPH performs worse in regard to winter precipitation and dryer areas than TRMM against CN05.1. Although ERA5 behaves better with integrated properties compared with ERA-Interim and EARS-CMA over East Asia, EARS-CMA produces more reliable annual, summer and winter mean precipitation pattern than ERA5 over the subregions dominated by large scales in mainland China, including the Tibetan Plateau and northwestern China, similar to its driving fields, ERA-Interim. In addition, the improvement from ERA-Interim to EARS-CMA can be obtained in reasonably reproducing precipitation seasonality in South China, Indo-China and southern Japan. Thus, the compatibility of EARS is outstanding in maintaining the advantages of its corresponding driving fields, ERA-Interim, as well as developing finer small scales. Although slightly behind ERA5 in the subregions affected by tropical systems and monsoons, EARS-CMA is competitive in acting as reference data for daily, seasonal, annual and interannual precipitation estimations over mainland China.

KEY WORDS

East Asia, mainland China, precipitation, reanalysis data

1 | INTRODUCTION

Both observations and reanalysis are designed to produce a climate dataset with fine and accurate regional features. With the development of the assimilation system and climate model, atmospheric reanalyses have prominent advantages of spatial and temporal coverage over observational datasets by blending an enormous amount of station observations and providing long-term and high-resolution

datasets (Bojinski *et al.*, 2014; Bollmeyer *et al.*, 2015; Sun *et al.*, 2018). Compared with observation-gridded datasets, reanalysis data can provide various meteorological variables with climatic and synoptic time scales that are barely obtained directly from meteorological instruments, especially in regions with complicated natural conditions. Reanalysis datasets, therefore, have been widely applied as reference data in studies on synoptic processes, climate variability, climate change, and extreme weather events

(Rood and Bosilovich, 2010; Hu *et al.*, 2016; Blender *et al.*, 2017; Quinting and Vitart, 2019; Avila-Diaz *et al.*, 2020). It is essential to continue improving reanalysis data for climate validation, research and public services.

Many meteorological research institutes have been engaged in updating and upgrading reanalysis products, including Climate Forecast System Reanalysis (CFSR) from the National Centers for Environmental Prediction (NCEP) (Saha *et al.*, 2010), ERA5 atmospheric reanalysis (ERA5) from the European Centre for Medium-Range Weather Forecasts (ECMWF) (Hersbach *et al.*, 2020) and the Japanese 55-year Reanalysis (JRA-55) from the Japanese Meteorological Agency (Kobayashi *et al.*, 2015). The temporal and spatial resolutions of recent global reanalyses have been significantly improved, largely attributed to advances in data assimilation techniques and observing networks. For instance, ERA5, the state-of-the-art global reanalysis based on the ensemble 4D-Var data assimilation system, can produce various atmospheric variables with a 31 km resolution for subdaily variability at 137 levels back to 1950. Although the resolution of the latest global reanalyses has markedly improved, obstacles are still present for global reanalysis systems to resolve the mesoscale processes over a specific region (Dulière *et al.*, 2011; Moore and Renfrew, 2014; Jiang *et al.*, 2020). Fortunately, an efficient solution, dynamic downscaling, has been undertaken to generate local-scale features for global reanalysis systems.

Dynamical downscaling retains errors from the driving global analyses at the lateral boundary and systematic model errors, which can be largely suppressed with the assimilation of regional observations (Dulière *et al.*, 2011; Bromwich *et al.*, 2016; Whelan *et al.*, 2018). The high-resolution regional climate model with data assimilation, that is, regional reanalyses, have been successfully applied to regional weather and climate studies in North America (Mesinger *et al.*, 2006), Europe (Bollmeyer *et al.*, 2015; Dahlgren *et al.*, 2016), the polar region (Bromwich *et al.*, 2011; Bromwich *et al.*, 2016) and Australia (Su *et al.*, 2019) with more reliable performance for most meteorological variables than global reanalyses, especially in complex regions. Recently, the 2 km reanalysis for Central Europe (COSMO-REA2) has even reached convection-permitting resolution, which significantly improves the representation for frequencies of local precipitation and spatial consistency over Germany compared with coarser global reanalyses (Wahl *et al.*, 2017).

As one of the classic monsoon regions in the world influenced by the world's highest plateau, the Tibetan Plateau, East Asia suffers from complex regional-scale climate variability, which is rarely captured in a global reanalysis system (Kang *et al.*, 2002; Gao *et al.*, 2006; Hwang *et al.*, 2018). Some competitive regional reanalyses have

been carried out by using advanced assimilation systems in East Asia. China Regional Reanalysis (CNRR) has an outstanding advantage in simulating precipitation, temperature and regional extreme events in mainland China in 2013 over the classic regional model by applying a gridpoint statistical interpolation (GSI) assimilation system (Zhang *et al.*, 2017). Another two new assimilation systems are also available for test periods no longer than 2 years over areas focusing on the Tibetan Plateau and Korea (Yang and Kim, 2017; He *et al.*, 2019). However, few efforts have been made on a regional reanalysis system covering a long-term period over all of East Asia. Due to limited temporal and spatial coverage, the regional reanalyses in East Asia are far from implementation and application in climate forecasting and model simulation compared with those in Europe and North America. Thus, it is urged to establish a continuous high-resolution regional reanalysis with long-term simulation for describing the local climate in East Asia in detail, which can contribute not only to the cooperation of meteorological research institutes but also the development of convective-permitting climate models in East Asia.

To fill the gap between East Asia and other regions around the world, the China Meteorological Administration has conducted a national research project since 2018 to establish a high-resolution regional reanalysis system over East Asia (Yin *et al.*, 2018). Recently, a 10-year East Asia regional reanalysis system (EARS-CMA) employing the Weather Research and Forecast (WRF) model (Skamarock *et al.*, 2008) has been successfully released. Before implementation and application, assessing data quality is a necessary task to ensure the consistency between the new assimilation system and other well-approved observation or reanalysis datasets. As an essential indication of climatological states, precipitation can reflect the complex nonlinear interaction between model parameterizations and represent the model's ability. Many studies have shown that the precipitation simulated by regional climate models tends to be overestimated and does not behave well in terms of seasonality and the diurnal cycle due to systematic bias in East Asia, especially for long-term simulations (Ding *et al.*, 2006; Huang *et al.*, 2013). Thus, it is important to evaluate different timescale- and spatial-scale features of precipitation of EARS-CMA in East Asia.

Benefiting from near-global coverage, satellite-based products are as popular as reanalysis data in various hydrological studies. To facilitate the evaluation of precipitation at subdaily timescales, it is crucial to quantify the characteristics of satellite-based products in specific regions due to their uncertainties. Our objectives are (a) to compare popular satellite- and reanalysis-based datasets with gauge-based data to provide useful information for the choice of the most appropriate observational

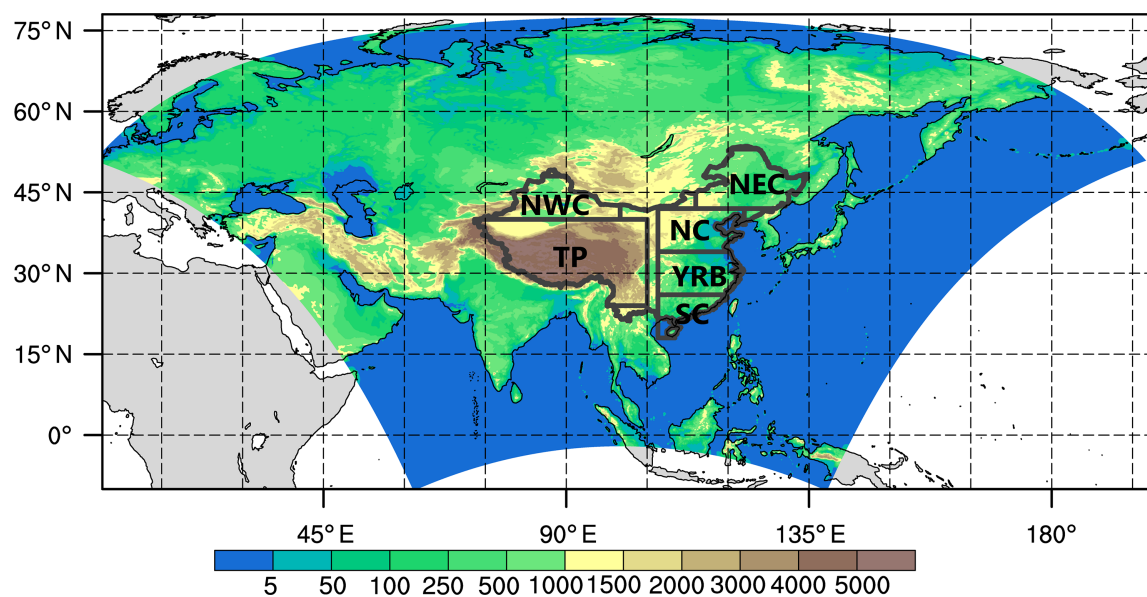


FIGURE 1 The WRF model domain for EARS-CMA reanalysis. Seven subregions are denoted with thick lines, including China mainland, northeast of China (NEC, 42°–53° N, 114°–134° E in China mainland), North China (NC, 34°–42° N, 107°–123° E in China mainland), Yangtze River basin (YRB, 26°–34° N, 107°–123° E in China mainland), South China (SC, 18°–26° N, 107°–123° E in China mainland), the Tibetan plateau (TP, 24°–40° N, 73°–105° E in China mainland) and northwest of China (NWC, 40°–48° N, 77°–100° E in China mainland) [Colour figure can be viewed at [wileyonlinelibrary.com](#)]

or reanalysis product for climate and hydroclimatic studies in East Asia, especially mainland China, and (b) to assess the quality of EARS-CMA and the development from ERA-Interim to EARS-CMA. This article is organized as follows. In Section 2, the regional reanalysis, observation and global reanalysis data assimilation systems are described. In Section 3, we assess the spatial characteristics of precipitation followed by the temporal evolution of rainfall in Section 4. Finally, the conclusions are provided in Section 5.

2 | REANALYSIS DESCRIPTION

2.1 | Model configuration and methodologies

The EARS-CMA reanalysis system was established utilizing the WRF model Version 3.9.1 coupled with the gridpoint statistical interpolation (GSI) data assimilation system, which has been widely applied in Asian regional climate research (Xu *et al.*, 2009; Yang *et al.*, 2015; Zakeri *et al.*, 2018). The model domain is centred at 38° N, 100° E with 900 × 760 grid points covering all of East Asia, South Asia and most parts of central Asia (Figure 1). In the vertical direction, 74 sigma levels up to 10 hPa are layered, and the horizontal resolution is 12 km. Based on numerous sensitivity experiments (Yin *et al.*, 2014; Li *et al.*, 2018), the model physics options

chosen in the study include the Kain (2004) cumulus parameterization scheme, the new Thompson micro-physics scheme (Thompson *et al.*, 2008), the rapid radiative transfer model (Iacono *et al.*, 2008) for both shortwave and longwave radiative schemes, the Yonsei University planetary boundary layer scheme (Hong *et al.*, 2006), the MM5 Monin–Obukhov similarity surface layer scheme (Janjic, 1994), and the Noah land surface model with multiparameterization options (Noah–MP) (Niu *et al.*, 2011). Initial and boundary conditions for EARS-CMA are provided by 6-hr ERA-Interim reanalysis data (Dee *et al.*, 2011) with a $0.75^\circ \times 0.75^\circ$ spatial resolution.

To illustrate the regional precipitation features in mainland China clearly, the model domain is separated into seven subregions, including mainland China, Northeast China (NEC, 42°–53° N, 114°–134° E in mainland China), North China (NC, 34°–42° N, 107°–123° E in mainland China), Yangtze River Basin (YRB, 26°–34° N, 107°–123° E in mainland China), South China (SC, 18°–26° N, 107°–123° E in mainland China), the Tibetan Plateau (TP, 24°–40° N, 73°–105° E in mainland China) and Northwest China (NWC, 40°–48° N, 77°–100° E in mainland China) (Figure 1). To measure the differences between each reanalysis dataset and the referenced data, the Taylor diagram is applied with the calculated root mean square error (RMSE), correlation coefficient, relative bias, and standard deviation (SD) (Taylor, 2001).

2.2 | Data assimilation technique and observations

From 1800 UTC on December 31, 2007 to 0000 UTC on January 1, 2018, EARS-CMA was updated four times a day (at 0000, 0600, 1200, and 1800 UTC) with a 12-hourly assimilation window and provided hourly output every day. At each cold start, all observations in the planetary boundary were not assimilated with the GSI system in EARS-CMA to avoid possible uncertainties induced by assimilated observations near the surface (Bédard *et al.*, 2015; Pu, 2017). During each model assimilation process, the surface observation nudging was active by approaching temperature, relative humidity and horizontal winds (Alapaty *et al.*, 2008), which passed quality control and was produced by the WRF's preprocessing objective analysis (OBSGRID) module. More importantly, the first 6 hr in each assimilation process are deemed the spin-up period, while the ninth and twelfth hours are used as first-guess fields, which are assimilated with the radar observations provided by the 3D-Var technique and cloud analysis in the GSI system. By blending more than 2,400 observational stations, 120 radiosonde stations and all available radar data over mainland China, EARS-CMA is supposed to provide high-quality and credible data at fine temporal and spatial resolutions.

To identify the improvement from ERA-Interim to EARS-CMA, 6-hourly ERA-Interim with a $0.75^\circ \times 0.75^\circ$ spatial resolution is employed as one of the global analyses compared with the new EARS-CMA. Another chosen global reanalysis data is the hourly ERA5 reanalysis at a 25 km resolution, which represents the state-of-the-art global assimilation system and has been widely applied and accepted in climatological research over East Asia (Gui *et al.*, 2020; Lei *et al.*, 2020; Yao *et al.*, 2020). For validation and comparison with reanalysis datasets, three observation-gridded products of precipitation are applied, including the Tropical Rainfall Measuring Mission (TRMM) 3B42V7 product (Huffman *et al.*, 2007), Climate Prediction Center (CPC) MORPHing technique (CMORPH) bias-corrected product (CMORPH, Joyce *et al.*, 2004) and CN05.1 (Wu and Gao, 2013). All observations have $0.25^\circ \times 0.25^\circ$ spatial resolutions and provide daily precipitation in 2008–2017 over the East Asia domain. As the most comprehensive station-based gridded dataset in China, CN05.1 based on 2,416 observational stations has been widely used for calculating historical climate change and validating model performance (Wu *et al.*, 2017; Yang *et al.*, 2019; Zhu and Yang, 2020). Focusing on mainland China, CN05.1 is used as the main reference dataset for the evaluation of precipitation over the subregions. In particular, TRMM shows more credible spatial and temporal features for precipitation than

CMORPH over all subregions in the next sections. Considering the temporal resolution of CN05.1 and the assessment results, the 3-hourly satellite-based TRMM data are applied as the reference dataset for diurnal cycle comparison.

3 | SPATIAL CHARACTERISTICS OF PRECIPITATION

In this section, we start the assessment with the comparison of the spatial pattern of annual mean precipitation over East Asia ($5^\circ\text{--}55^\circ\text{ N}$, $70^\circ\text{--}140^\circ\text{ E}$) among the three observations and three analyses (Figure 2). Overall, the spatial distributions of the 10-year mean precipitation from the six datasets are similar to each other in mainland China, with a decrease from southeast to northwest. For the three observations, CMORPH underestimates the rainfall over the TP region compared with CN05.1 and TRMM. Comparably, ERA-Interim represents the worst annual mean rainfall amount with a large rainfall centre in Sichuan Province in southwestern China against the three observations among the three reanalysis datasets. Focusing on the contrast between ERA-Interim and EARS-CMA, it is clear that EARS-CMA corrects the overestimation of precipitation over Sichuan Province in China and northwestern Indo-China. Additionally, EARS-CMA enhances the rainfall belt south of Japan associated with the Meiyu rainfall band compared with ERA-Interim, although it represents the largest rainfall amount over the ocean due to the effect of the lateral boundary and parameterization. Although the main rainfall belts from EARS-CMA are more intense than ERA5, the pattern of EARS-CMA resembles ERA5, CN05.1 and TRMM well. It is important to note that the regional reanalysis, EARS-CMA, can produce finer features of precipitation on land than ERA-Interim can, especially for the monsoon-related region, and its ability is close to the ensemble-based ERA5.

The seasonal performance of different analyses can be evaluated by the seasonal average and seasonality of precipitation obtained from the difference between the summer (June–July–August, JJA) mean and winter (December–January–February, DJF) mean pattern (Figure 3). Affected by the monsoon, the precipitation exhibits distinct seasonal variation on land over East Asia with wet summers and dry winters. For the three observations, their JJA mean and seasonality of precipitation distribution are quite similar, while the TRMM and CMORPH present less rainfall over SC in winter than CN05.1, especially CMORPH (Figure 3a). The similarities of seasonal rainfall centres between ERA5 and EARS-CMA can be easily found in the summer and seasonality rainfall pattern as two separate rain belts in China

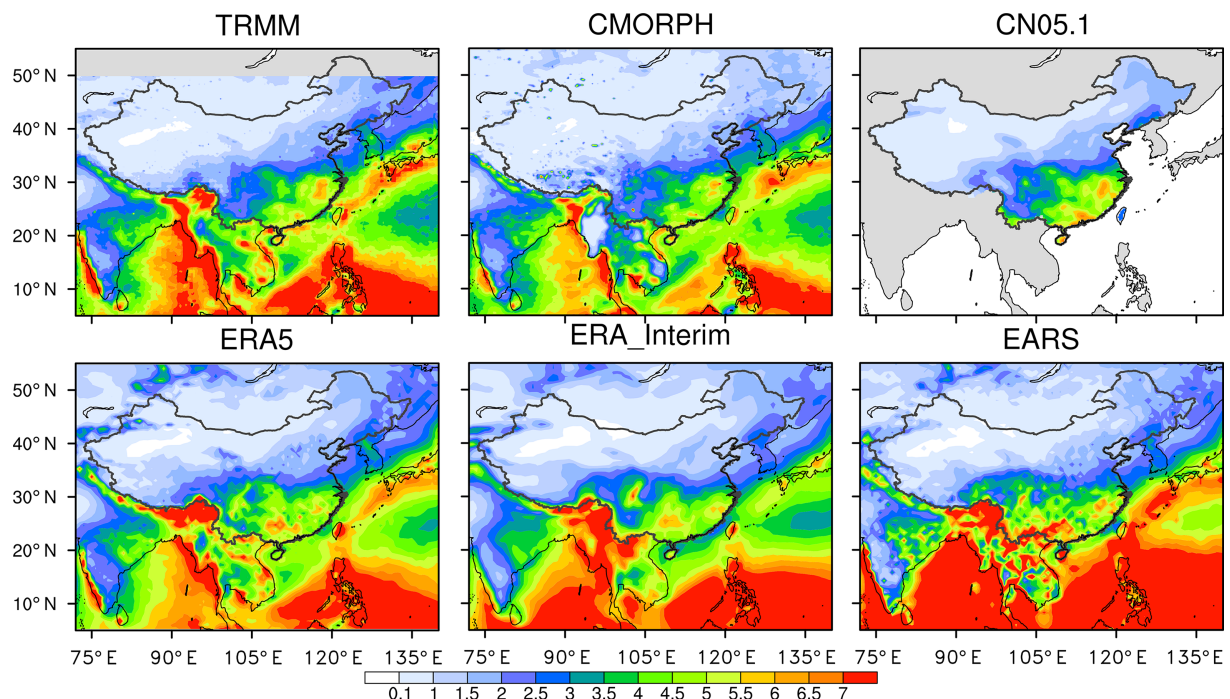


FIGURE 2 Spatial distribution of annual mean precipitation over East Asia in 2008–2017 (unit: mm/day) [Colour figure can be viewed at wileyonlinelibrary.com]

corresponding to the Meiyu front near 30° N and located in the region at approximately 20° N that is affected by tropical systems, terrain and monsoon along the southern slope of the Himalayas to southern China, which are quite consistent with the observed distributions (Figure 3b). On the other hand, the main summer rainfall of ERA-Interim over YRB is located south of 30° N and tends to be underestimated by approximately 1 mm/day north of 30° N, resulting in weaker seasonality precipitation over YRB than ERA5 and EARS-CMA (Figure 3b). It is clear that ERA-Interim provides the worst performance for rainfall over SC, YRB and western Indo-China in both summer and winter among the three reanalyses. On the East China Sea and south of Japan, the seasonal cycle amplitude of precipitation from EARS-CMA is larger than that of ERA5 and ERA-Interim but closer to the observations, indicating more reasonable movement of monsoons over East Asia in EARS-CMA. Obviously, the improvement in the location of rainfall centres over SC, YRB, western Indo-China and East China Sea from ERA-Interim to EARS-CMA indicates that the regional assimilation system is capable of reproducing seasonal variation in precipitation and monsoon variability.

Since the precipitation over different subregions varies considerably in China, we use the root mean square error (RMSE), correlation coefficient (R), relative bias (RB), and standard deviation (SD) to quantify the difference in the annual, summer and winter mean precipitation among the three reanalysis datasets over seven

specific subregions against CN05.1, shown as Taylor diagrams in Figure 4. When $R < 0$ or $SD > 1.65$, the corresponding statistics are depicted at the bottom of each subfigure. It is clear that the three reanalysis datasets have better performance and show small differences in reproducing annual and winter precipitation than summer precipitation over most subregions. In NWC and TP, ERA-Interim and EARS-CMA present larger R and smaller RB values than ERA5 for annual, summer, and winter precipitation, indicating the strong influence of driving fields on the large-scale processes in WRF over the subregions controlled by westerlies, which can benefit from observation nudging as well. All reanalysis datasets do not perform well over SC, with ~15% overestimation in summer and 10% underestimation in winter, but EARS-CMA has larger spatial Rs for annual, JJA and DJF rainfall than both ERA5 and ERA-Interim. However, the summer and annual mean precipitation from EARS-CMA represent smaller R values by ~0.1 and larger SD values by over 0.05 than the other two reanalysis datasets in NEC. It can be concluded that the performance of the reanalysis dataset shows strong dependence on the region of interest. However, in general, EARS-CMA shows a competitive ability in reproducing the spatial structures of annual and seasonal precipitation over various subregions in China.

To reveal the intensity of precipitation events over different subregions, we classify the region-averaged rainfall

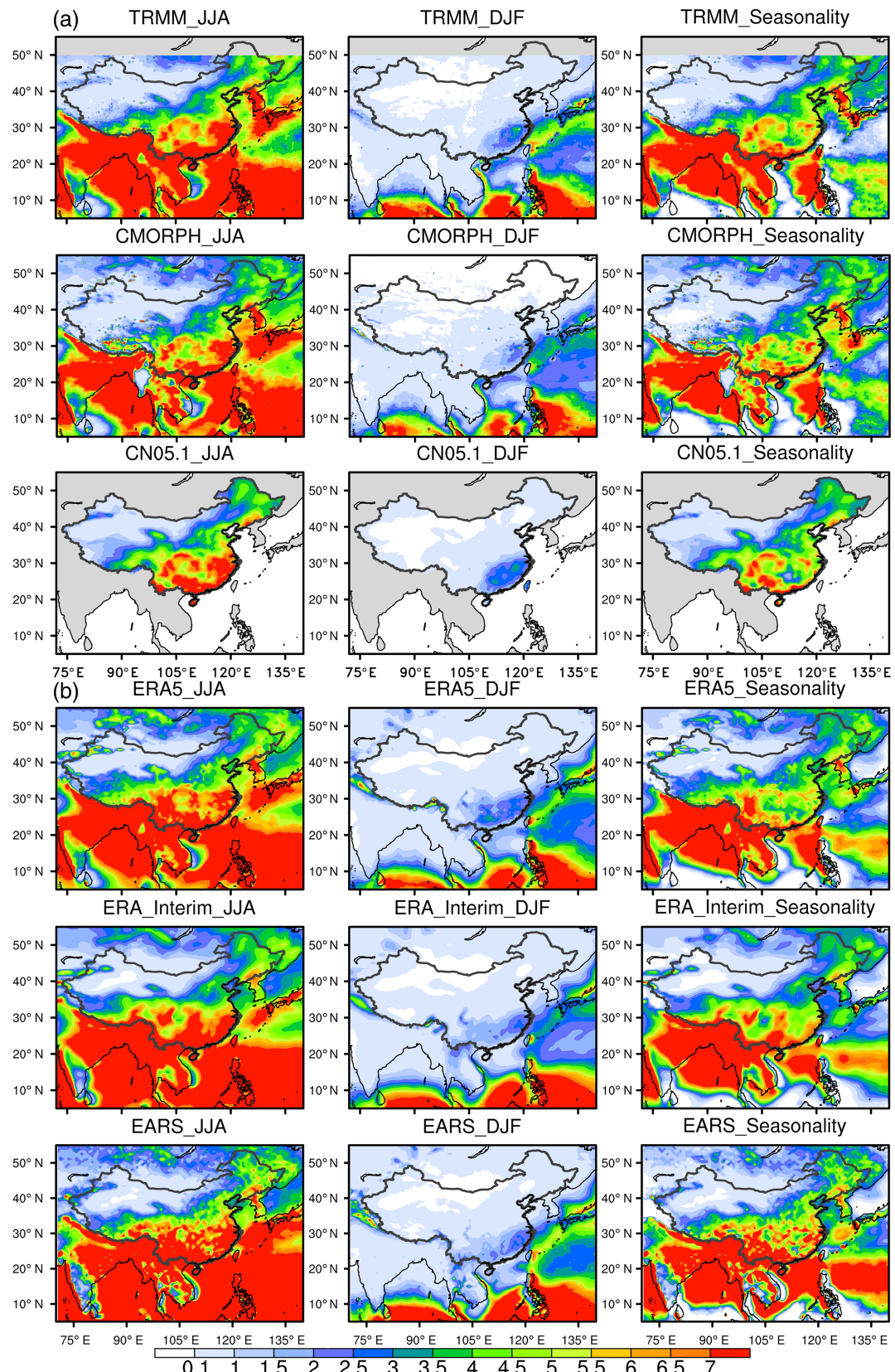
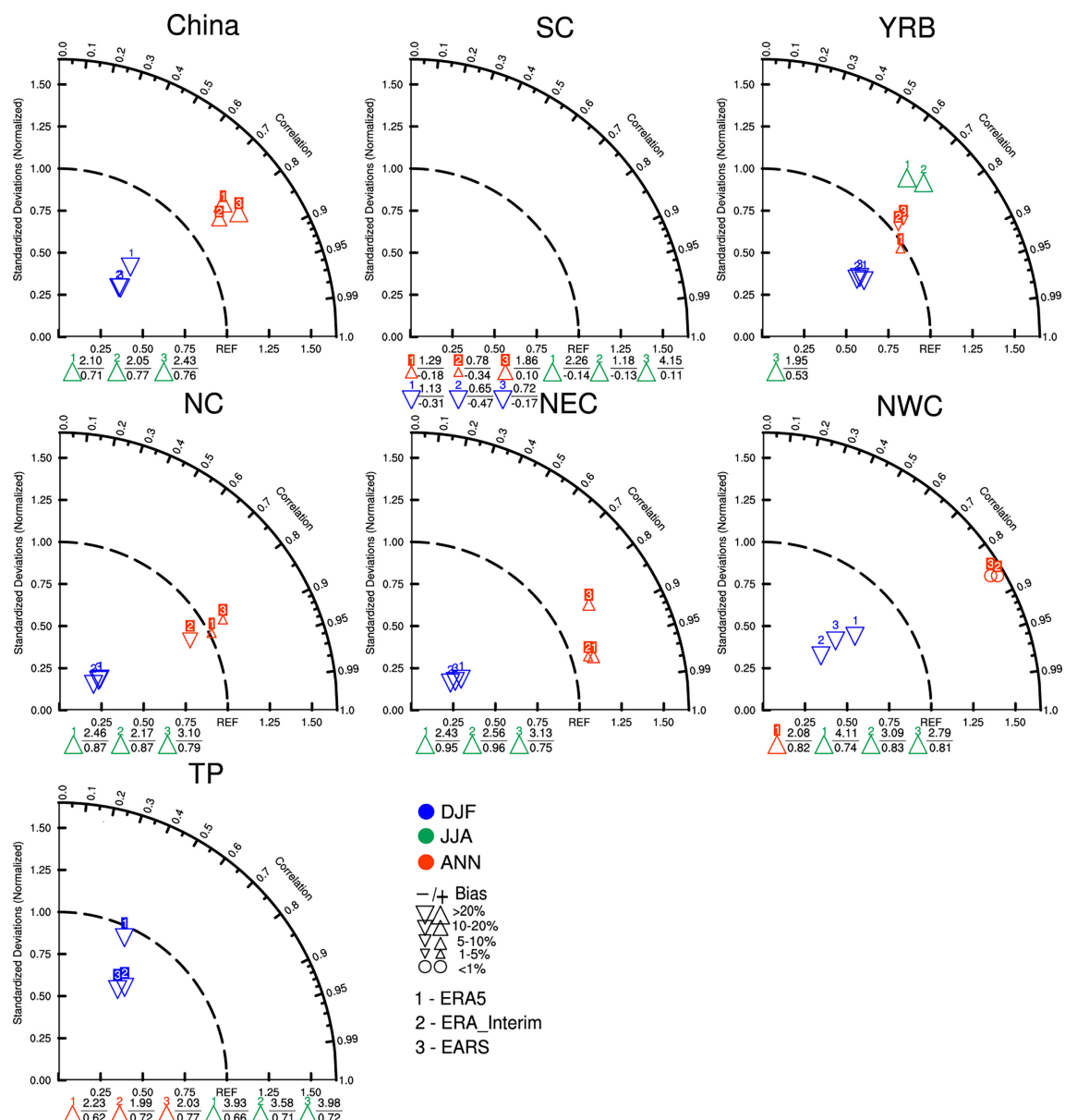


FIGURE 3 The spatial distribution of summer, winter mean and the seasonality precipitation over East Asia in 2008–2017 (unit: mm/day). (a) Observations, (b) reanalysis data [Colour figure can be viewed at wileyonlinelibrary.com]



events according to daily rainfall amount into different categories, as shown in Figure 5. To describe simply and efficiently, we identify four precipitation grades as drizzling (0.1–1 mm/day), light (1–5 mm/day), medium (5–10 mm/day), heavy (10–20 mm/day) and extreme (>20 mm/day) rainfall. The daily rainfall intensity of the three reanalysis datasets is reasonable and close to observations in most parts of mainland China, except for SC, YRB and TP. Comparing the three analyses against CN05.1 and TRMM, the climate

model with a resolution larger than 20 km still hardly resolves small scales and orographic drag in complex terrain, leading to overestimation of the occurrence of drizzling rainfall and overestimation of medium precipitation by $\sim 10\%$ and 5%, respectively, over the TP. In SC and YRB, things are much more complicated. The frequencies of the seven categories from EARS-CMA are closer to TRMM in the YRB than ERA-Interim and ERA5. However, compared with CN05.1 in the YRB, EARS-CMA underestimates the frequency of

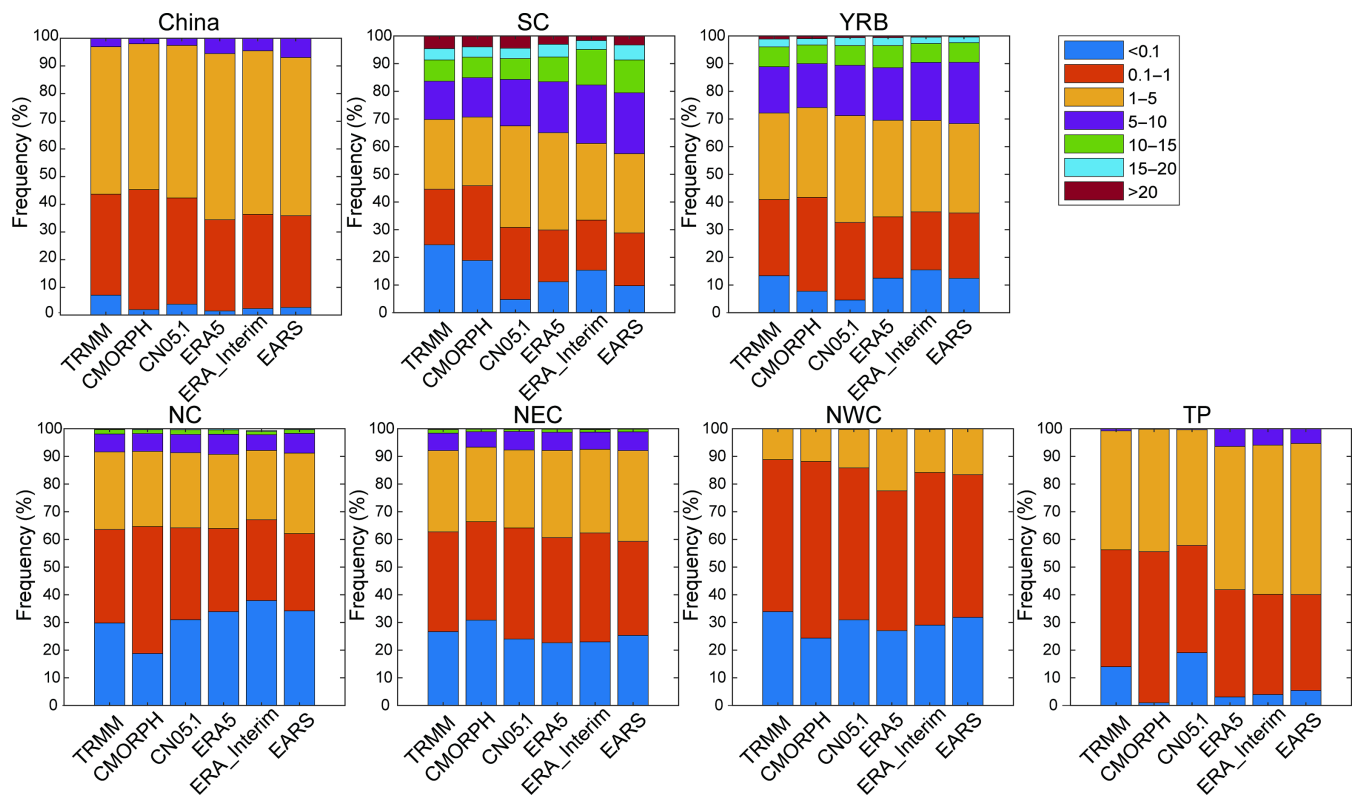


FIGURE 5 The frequency for different intensity categories of rainfall events over seven subregions in 2008–2017. The unit of intensity categories is mm/day; the unit of frequency is % [Colour figure can be viewed at wileyonlinelibrary.com]

drizzling rainfall by 5%. It can be inferred that the referenced dataset can impact the evaluation results.

With the gamma distribution function, the cumulative probability distributions are calculated for the region-averaged daily precipitation in the summers and winters of 2008–2018 (Figure 6). CMORPH shows poor skill in reproducing drizzling DJF rainfall over the dryer areas with the farthest deviation from the other two observations, including NC, NEC, NWC and the TP. In mainland China, the reanalysis datasets tend to produce less medium rainfall than the observations by ~5% for both JJA and DJF precipitation. Comparing EARS-CMA and ERA-Interim, the spectrum of EARS-CMA is consistent with ERA-Interim for winter precipitation over all subregions and for summer rainfall over most subregions. This indicates that the driving field can contribute to the performance of the daily precipitation rainfall intensity of EARS-CMA, especially in the subregions or in a period controlled by westerlies. In addition, for summer precipitation, the appearance of drizzling, light and medium rainfall in EARS-CMA is lower than in other reanalysis datasets and observations over SC and the YRB by ~10% due to the more frequent occurrence of heavy rainfall, which indicates that the added small scales in the regional model, WRF, can lead to more heavy rainfall events for the subregions influenced by both monsoon and synoptic systems.

4 | TEMPORAL CHARACTERISTICS OF PRECIPITATION

After the assessment of spatial features, we turn to the reanalysis of the temporal evolution of precipitation at various time scales. The interannual variation in subregion mean monthly rainfall is depicted in Figure 7, which is standardized by the monthly mean climatology precipitation of individual datasets in 2008–2017. The year-to-year curves of the observed and reanalysis datasets represent more remarkable differences since 2012 than before 2012. For mainland China, the three reanalysis datasets obviously deviate from the three observations in 2013, when China suffered substantially from precipitation extremes. It is difficult to identify which is better or more accurate among the observations and analyses compared with CN05.1. However, the curve of interannual CMORPH rainfall is further from CN05.1 than TRMM and even the three reanalyses with the smallest correlation coefficients, 0.93, 0.71 and 0.70, over NEC, NWC and TP, indicate that more caution should be given in the application of CMORPH in dryer areas. Obviously, the trends and correlation coefficients of EARS-CMA are close to ERA-Interim in all seven subregions, emphasizing the significant influence of driving fields, but a smaller rainfall bias during

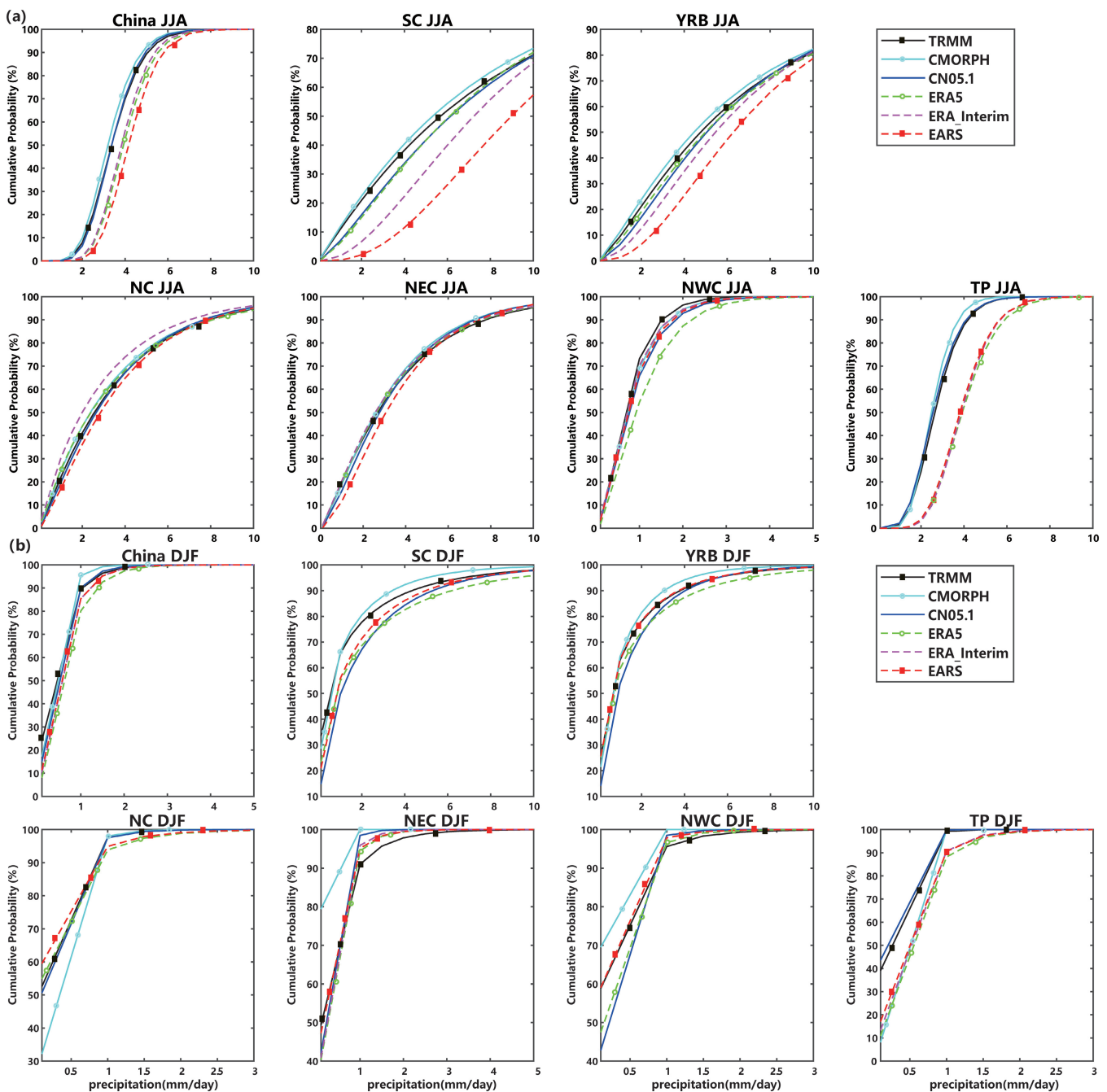


FIGURE 6 Cumulative distribution function of daily region-averaged precipitation based on gamma distributions for three observations and analyses over seven subregions in the JJA and DJF of 2008–2017 [Colour figure can be viewed at wileyonlinelibrary.com]

2012–2014 and larger correlations of EARS-CMA can still be found over monsoon-related subregions than ERA-Interim against CN05.1, including SC, YRB and NC.

To investigate the model's ability to recreate monthly change, Figure 8 represents the annual cycle of the region-averaged rainfall in 2008–2017 over different subregions. Comparing the six datasets, it can be easily seen that the three reanalyses can capture the features of the precipitation annual cycle, whereas they tend to create wetter months than CN05.1, CMORPH

and TRMM, particularly in summer over China. Additionally, in NWC and TP, the reanalyses do not perform as well as in other subregions. ERA5 provides the largest overestimation for summer rainfall of the annual cycle over NWC and TP among the reanalysis datasets compared with CN05.1. Although the results of EARS-CMA produce wetter summers than the other two reanalysis datasets, EARS-CMA can reflect the monthly variation in precipitation over SC and NC more reasonably than ERA-Interim. For instance, in SC, the rainfall from

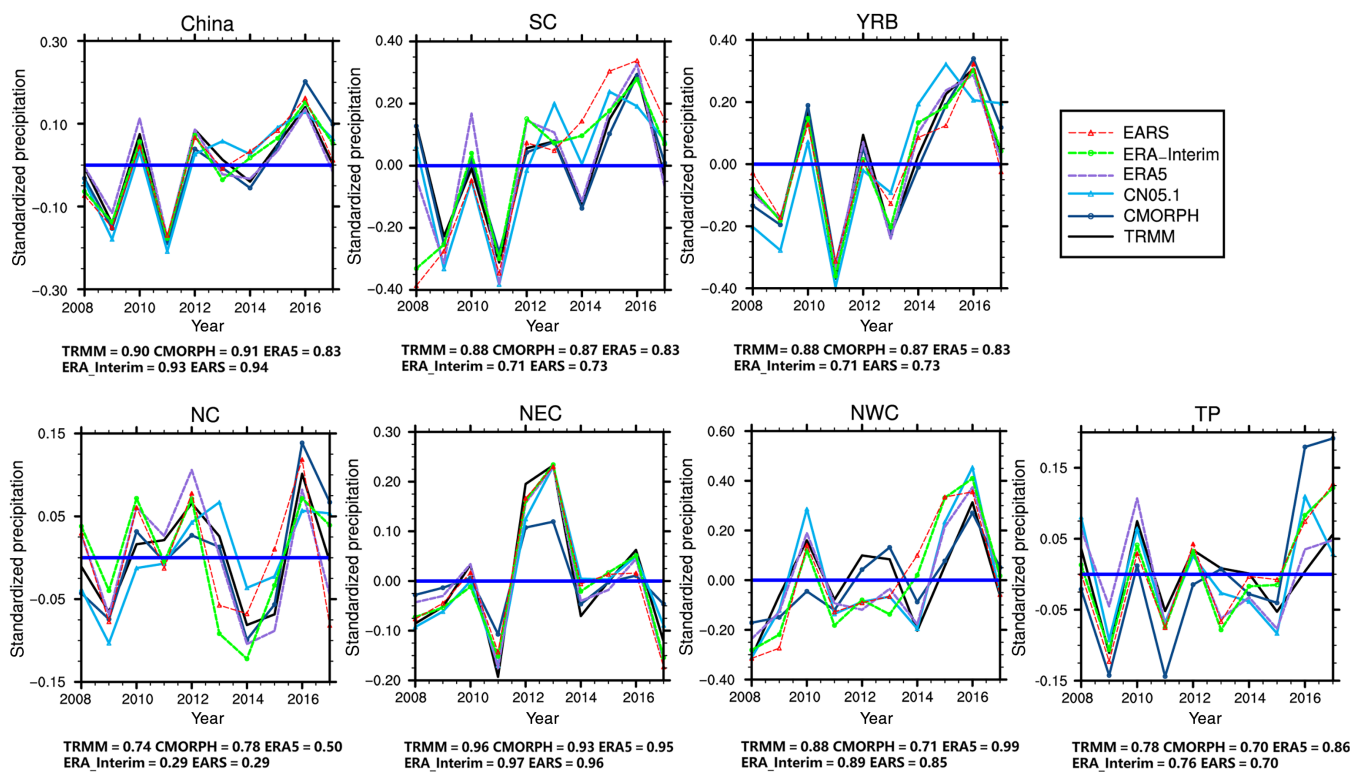


FIGURE 7 The interannual variation for region-averaged precipitation of the observations and reanalyses over seven subregions. The texts at the bottom of the subplot represent the correlation coefficients of the curves against CN05.1 [Colour figure can be viewed at wileyonlinelibrary.com]

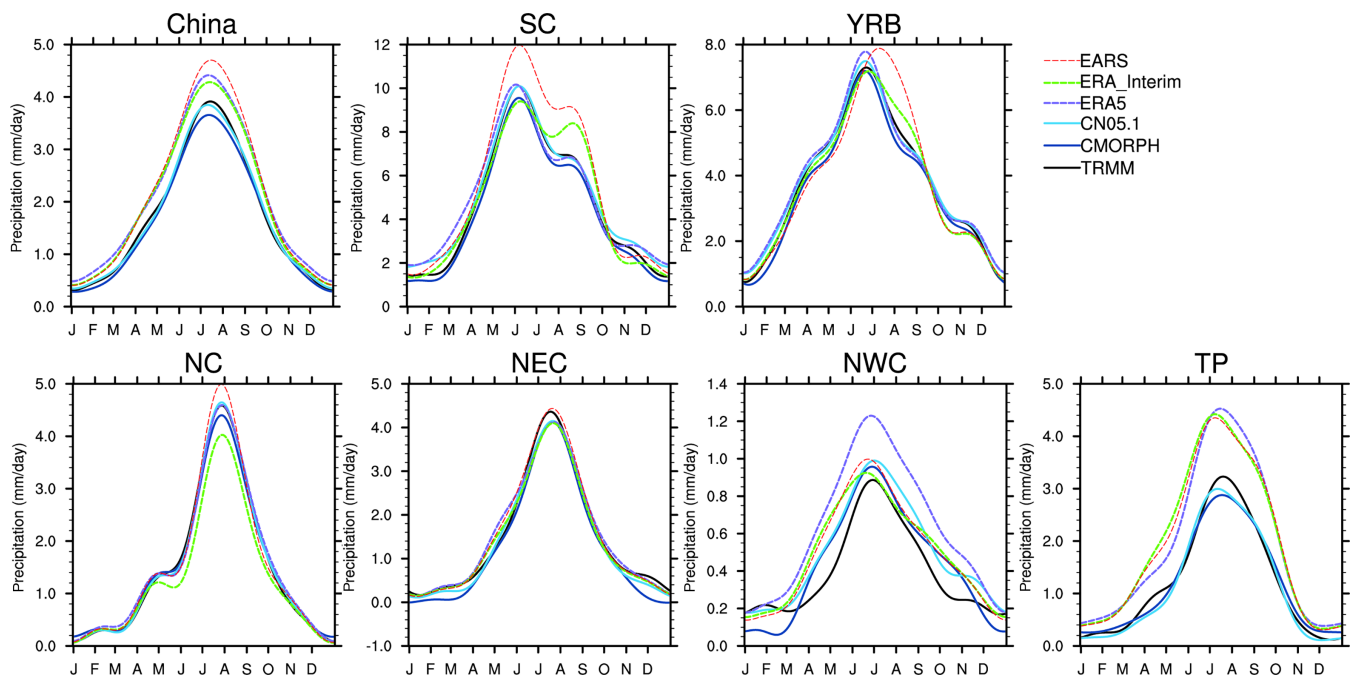


FIGURE 8 The annual cycle for region-averaged precipitation of the observations and reanalyses over seven subregions in 2008–2017 [Colour figure can be viewed at wileyonlinelibrary.com]

May to September based on EARS-CMA is significantly larger than the observations, but EARS-CMA appears to have a greater amplitude between the first rain peak in

early June and the second peak in middle August than ERA-Interim, which may benefit from a more reasonable migration of the monsoon.

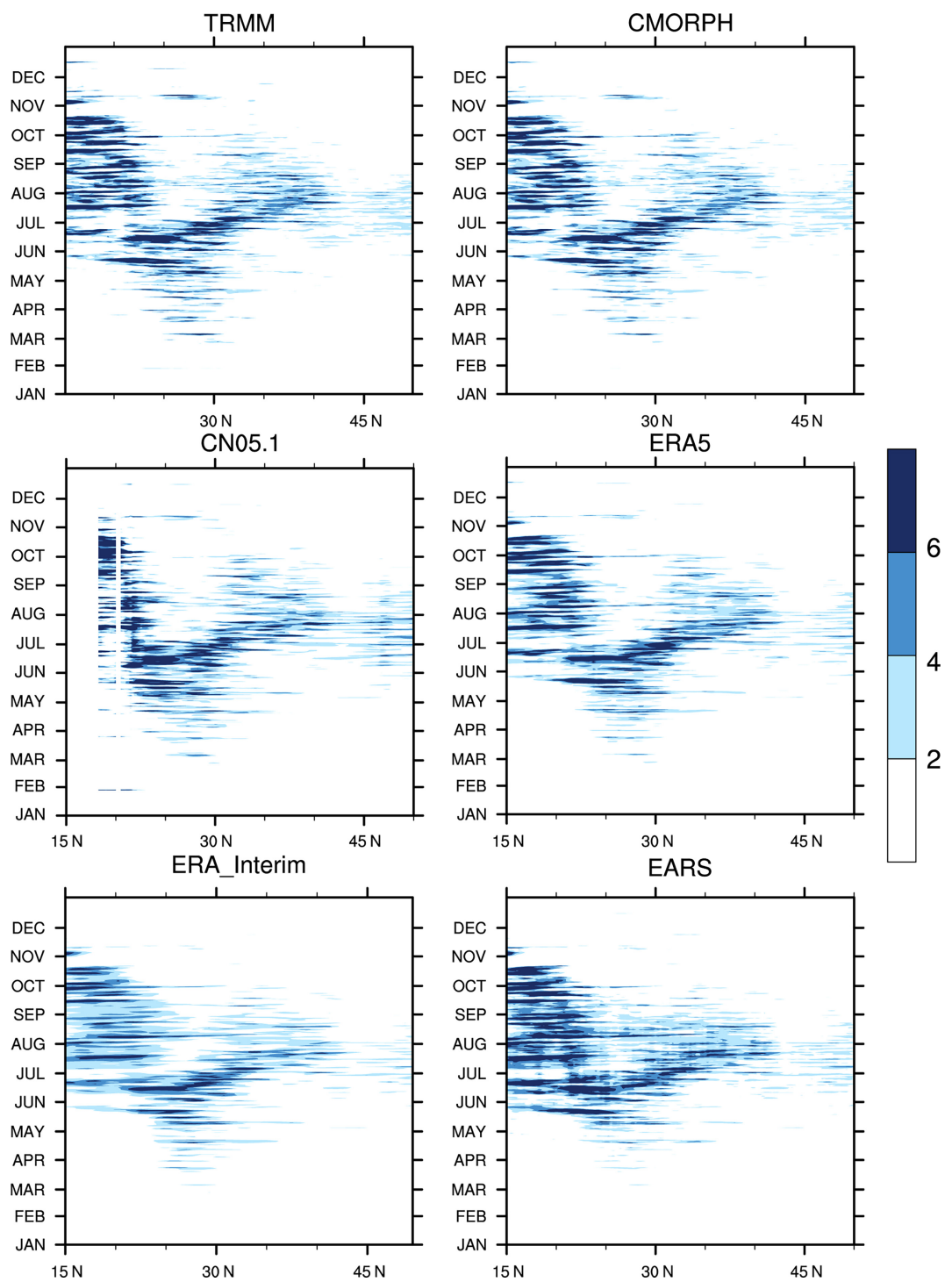


FIGURE 9 The Hovmöller diagram for major East Asia monsoon region-averaged (107° – 123° E) precipitation anomaly of the observations and reanalyses in 2008–2017 (unit: mm/day) [Colour figure can be viewed at wileyonlinelibrary.com]

As the seasonal variation in precipitation over China corresponds to the movement of East Asian monsoon systems to a large degree, we also focus on the migration of rainfall belts from different datasets averaged over eastern China between 107° E and 123° E, including SC, YRB and NC (Figure 9). All datasets present the shift of the monsoon-related rain belt from 15° N in late May, which

reaches the region at approximately 40° N in middle July. However, EARS-CMA exhibits the strongest northward progress and southward retreat between 15° N and 40° N, as shown by the obvious rainfall anomaly of up to 7 mm/day among the six datasets. As a result, the rainfall peak of the annual cycle over YRB from EARS-CMA occurs in early July, later than other reanalyses and

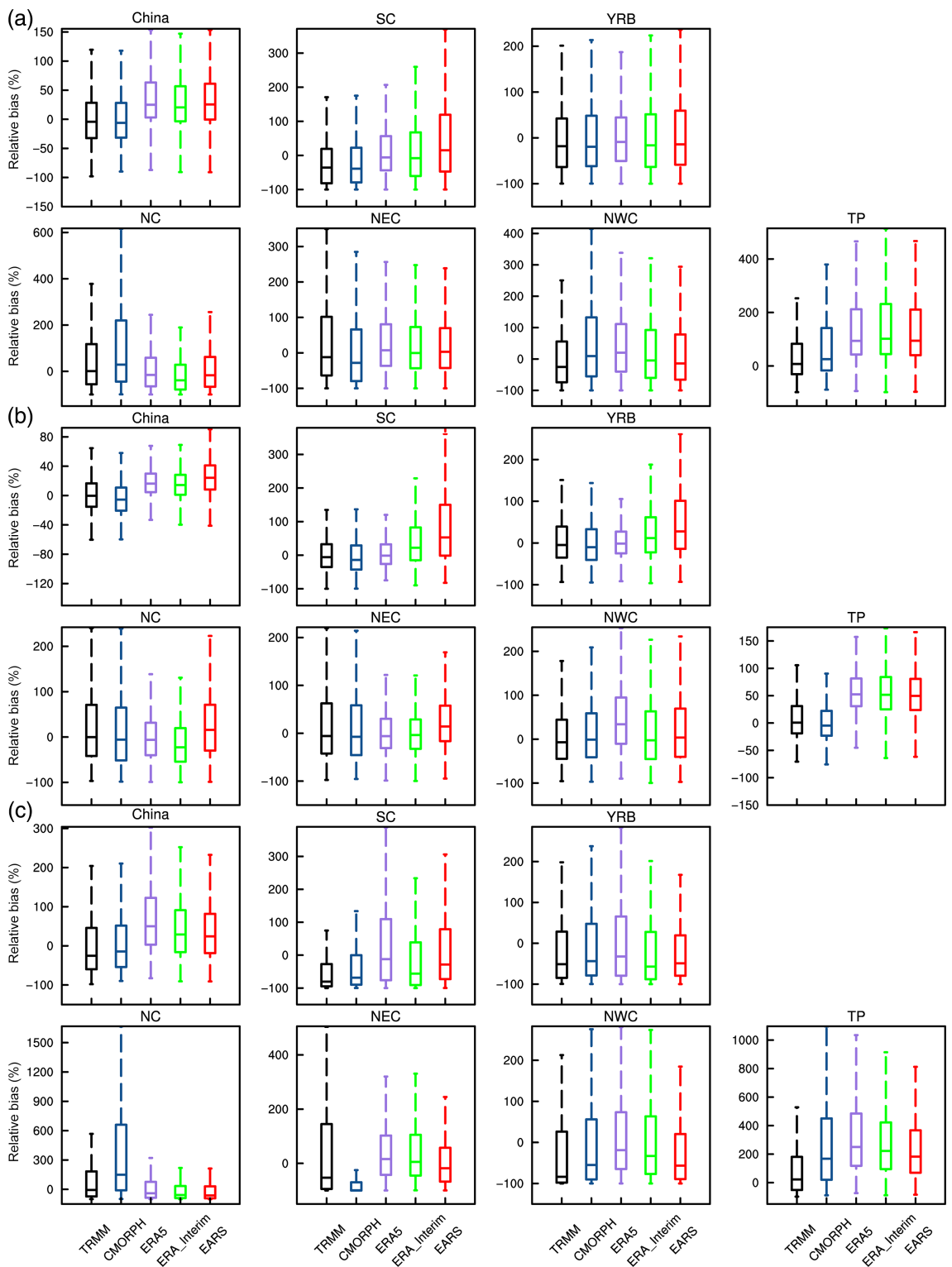


FIGURE 10 The box plot with the outliers removed for relative bias of daily region-averaged precipitation of the observations and reanalyses against CN05.1 over different subregions. (a) Annual precipitation, (b) summer precipitation, and (c) winter precipitation [Colour figure can be viewed at wileyonlinelibrary.com]

observations (Figure 8). Comparing EARS-CMA and ERA-Interim, a wetter SC can be found in EARS-CMA than in ERA-Interim from June to October, which leads to more reliable seasonal variation in Figure 8.

In addition, to investigate the performance of the six datasets over different subregions at the daily scale, box plots are employed to depict the daily relative bias for annual, JJA and DJF precipitation against CN05.1

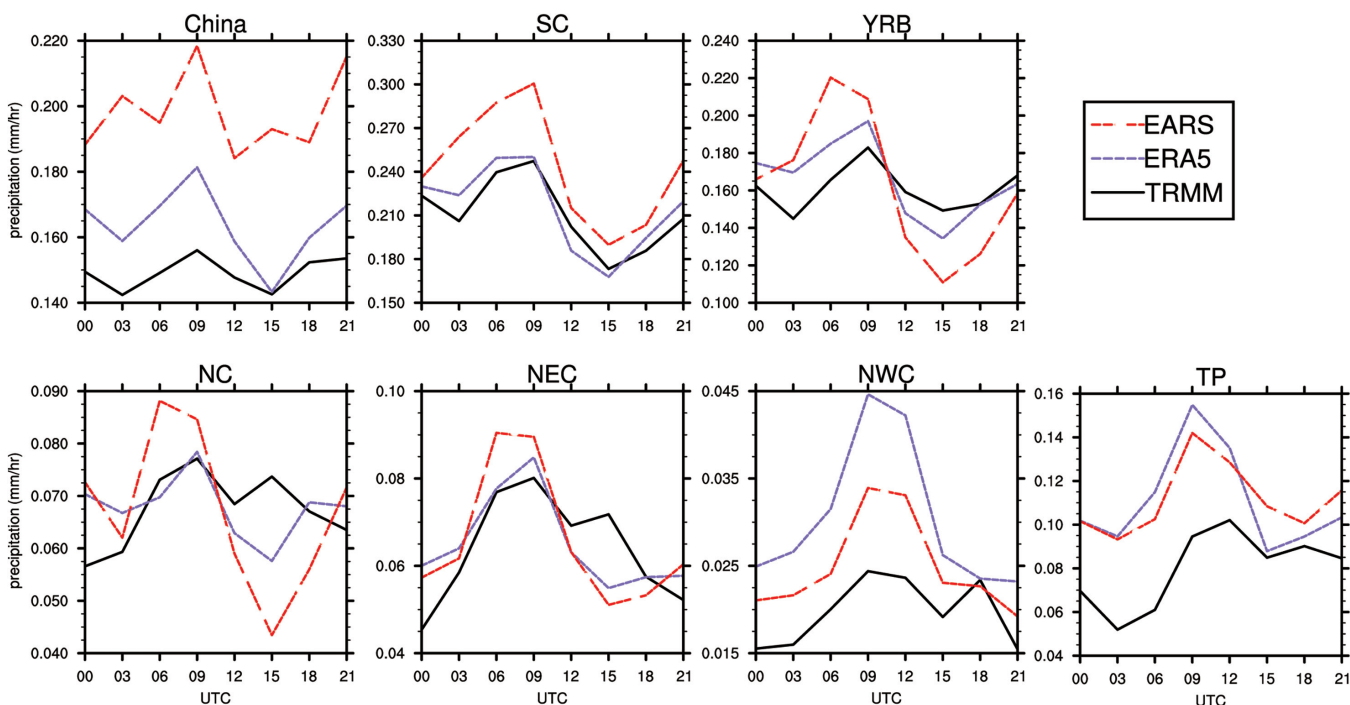


FIGURE 11 The diurnal cycle for region-averaged precipitation of EARS-CMA, ERA5 and TRMM over seven subregions [Colour figure can be viewed at wileyonlinelibrary.com]

(Figure 10). All datasets reflect wetter relative biases for the time series of daily rainfall across mainland China with respect to CN05.1. The relative bias of daily precipitation from CMORPH produces a more notable difference from CN05.1 over most parts of mainland China than TRMM, particularly in the winters of SC, NC and NWC, with ranges of $(-99.8\%, 133.7\%)$, $(-100.0\%, 1,665.7\%)$ and $(-88.7\%, 275.7\%)$, respectively. The 75th percentile minus the 25th percentile of relative bias from CMORPH is even larger than that of any other dataset over NC. Additionally, the estimation based on EARS-CMA indicates a wetter SC and YRB for annual and JJA daily precipitation but is closer to CN05.1 over NWC and TP than ERA-Interim. For winter daily rainfall, EARS-CMA appears to have fewer overestimates (with 75th percentile relative biases of 81.7%, 19.3%, 30.5%, 57.5%, 20.3% and 366.8% over mainland China, YRB, NC, NEC, NWC and TP, respectively) than other global analyses in most parts of mainland China except SC. It is clear that EARS-CMA can create an appropriate magnitude and regional discrepancy of daily rainfall in winter benefiting from the blending of station-observed data, which suppresses the overestimation of simulated precipitation from the WRF model and results in improvement in daily rainfall variation. In addition, the averages and range values (in brackets) of the relative biases of EARS-CMA in regard to annual, summer and winter precipitation of the TP region are 94.4% $(-96.5\% \text{ to } 467.0\%)$, 49.7% $(-61.8 \text{ to } 166.2\%)$, and 182.7% $(-84.7\% \text{ to } 812.4\%)$,

respectively. The EARS-CMA dataset is competitive in producing daily rainfall temporal features with the control of rainfall overestimation for mainland China, especially the TP region.

However, EARS-CMA does not demonstrate any superiority in reproducing the diurnal cycle over mainland China (Figure 11). Since the hourly precipitation provided by ERA-Interim comes from the forecast system and CMORPH does not perform as well in the above reanalysis as TRMM does, we compare the diurnal cycles of TRMM, ERA5 and EARS-CMA. TRMM acts as the reference dataset for the evaluation of the diurnal cycle of precipitation on mainland China. The diurnal cycle from TRMM represents one peak for region-averaged precipitation in mainland China, SC, YRB and TP, while it shows two peaks over NC, NEC and NWC. The occurrence time of the rainfall peak modulated by EARS-CMA matches the TRMM results in mainland China and SC, with overestimations of approximately 0.032 mm/hr and 0.23 mm/hr, respectively. However, for YRB, NC and NEC, EARS-CMA represents a peak time at 06:00 UTC, ~ 3 hr earlier than TRMM. When comparing the performance of EARS-CMA and ERA5 against TRMM, EARS-CMA outperforms ERA5 in reproducing the diurnal amplitude and amount of rainfall in NWC and TP. However, the magnitude and diurnal amplitude of 3-hourly average rainfall in ERA5 are more consistent with TRMM over SC and the YRB. This implies that with the assimilation technique, the ability of EARS-CMA

is nearly identical to that of ERA5 in producing the diurnal variation in rainfall in local regions in mainland China and even better than that of ERA5 in drier areas. However, ERA5 and EARS-CMA both miss the second peak of the diurnal cycle over NC, NEC and NWC. Therefore, the ability of reanalysis datasets to reproduce diurnal variation should be further improved, and may result from the error of processes resolved in the planetary boundary of a climate model.

5 | CONCLUSION AND DISCUSSION

In this article, we evaluate a new regional reanalysis with a 12-km resolution, EARS-CMA, in producing various scales of spatial and temporal features for precipitation over the East Asia domain by comparisons with two global reanalysis datasets, ERA-Interim and ERA5, and three observed datasets, CN05.1, TRMM and CMORPH. When comparing the performance of different reanalysis datasets, all reanalyses can capture the main characteristics of precipitation over different subregions with competitive abilities, but EARS-CMA can provide more detailed spatial features at timescales longer than 1 day.

There is no doubt that the performance of analyses can vary with the region of interest. Both ERA-Interim and EARS-CMA show an advantage over ERA5 for annual, JJA and DJF mean precipitation over the subregions significantly controlled by westerlies, whereas ERA5 produces the summer mean precipitation pattern best in NEC, YRB and NC. Additionally, ERA5 provides the largest overestimation for summer rainfall of the annual cycle over NWC and TP among the analyses against observations. In general, the significant influence of driving fields on a regional climate model has two sides: modulating the rainfall magnitude and frequency but undermining the local-scale processes, particularly with the nudging technique applied, which leads to the similar performance of EARS-CMA and ERA-Interim for most subregions at some time scales, such as interannual and annual variability. Therefore, it is essential for a regional reanalysis to maintain balance in handling the effects of driving fields and creating mesoscale processes.

Fortunately, EARS-CMA is superior to ERA-Interim in reproducing salient characteristics of monsoon-related rainfall bands with fine-scale spatial precipitation structures, particularly in summer, which illustrates that EARS-CMA can not only develop small scales freely but can also maintain the merits of corresponding driving fields. The prominent improvement in the seasonal precipitation pattern from ERA-Interim to EARS-CMA can be found over SC, YRB, western Indo-China and southern

Japan, implying the regional model's ability to provide local-scale processes and more accurate monsoon migration. More interestingly, the interannual variability of EARS-CMA shows improvements for bias and correlation than those from ERA-Interim during the period suffering from extremes against CN05.1 in the monsoon-related subregions, indicating that EARS-CMA may describe extreme precipitation events better, which needs to be further investigated. Unlike the tremendous overestimations of precipitation in traditional dynamic downscaling, it is clear that EARS-CMA produces reasonable rainfall intensity and frequency over all subregions, especially for winter daily precipitation, benefiting from the amalgamation of more than 10,000 station observations in the assimilation system, although it still modulates more frequent and intense heavy rainfall events accompanied by the strongest migration of monsoon rain bands in the subregions favoured by both monsoon and synoptic systems.

On the other hand, the performance of a reanalysis not only depends on the region but also the referenced dataset. At most times, the spatial and temporal features of the TRMM dataset are consistent with CN05.1, apart from drizzling rainfall, which may lead to a discrepancy in the assessment results. In the YRB, the frequency of various precipitation bins from EARS-CMA is the closest reanalysis to TRMM while underestimating drizzling rainfall compared with CN05.1. However, the poorest skill in regard to drizzling rainfall is obtained by CMORPH, which leads to an incredible distance from TRMM and CN05.1 in the reproduction of the daily evolution and frequency precipitation in winter. Since CMORPH tends to estimate less rainfall in drier subregions, especially in winter, we suggest applying CN05.1 and TRMM as observation data in China and East Asia, respectively, rather than CMORPH.

Thus, the properties of EARS-CMA show competitive advantages in daily precipitation estimation and seasonal, annual and interannual variations over East Asia. However, things have changed for diurnal variation. Both EARS-CMA and ERA5 can catch the diurnal cycle with one peak in China but have difficulty reproducing the regional diurnal variation featuring two peaks. This implies that more efforts should be devoted to boosting the reproduction of subdaily data in the reanalysis dataset.

As mentioned above, EARS-CMA can add finer and better precipitation features in the monsoon-related region than ERA-Interim. However, the "added" value has not been quantified in this study. Additionally, although this study found that EARS-CMA may create the feature of precipitation extremes better based on interannual variability, we have not delved deeply into its performance in regard to extreme precipitation events.

Since the added value is associated with extremes, we will discuss them in the next study to take a more comprehensive view of the performance of EARS-CMA.

AUTHOR CONTRIBUTIONS

Linyun Yang: Formal analysis; writing – original draft; writing – review and editing. **Xudong Liang:** Project administration; resources; supervision. **Jinfang Yin:** Data curation; resources; software. **Yanxin Xie:** Data curation. **Huiyi Fan:** Data curation.

ACKNOWLEDGEMENTS

This work was funded by the National Key R&D Program of China (2021YFC3000904), the Joint Funds of the National Natural Science Foundation of China (U2142214), the National Key Research and Development Program of China (2017YFC1501800) and the Basic Research Fund of Chinese Academy of Meteorological Sciences (2021Y030). We thank the European Centre, National Aeronautics and Space Administration, the Japan Aerospace Exploration Agency, National Oceanic and Atmospheric Administration and China Meteorological Administration for providing ERA-Interim, ERA5 reanalysis data, TRMM 3B42V7, CMORPH, CN05.1 for Research and Applications used in the research.

CONFLICT OF INTEREST

The authors declare no conflicts of interest.

DATA AVAILABILITY STATEMENT

The EARS-CMA data used during the study is available from the corresponding author by request. Open access to this dataset will be provided soon.

ORCID

Linyun Yang  <https://orcid.org/0000-0003-0887-8064>

REFERENCES

- Alapaty, K., Niyogi, D., Chen, F., Pyle, P., Chandrasekar, A. and Seaman, N. (2008) Development of the flux-adjusting surface data assimilation system for mesoscale models. *Journal of Applied Meteorology & Climatology*, 47(9), 2331–2350. <https://doi.org/10.1175/2008JAMC1831.1>.
- Avila-Diaz, A., Benezoli, V., Justino, F., Torres, R. and Wilson, A. (2020) Assessing current and future trends of climate extremes across Brazil based on reanalyses and earth system model projections. *Climate Dynamics*, 55(5), 1403–1426. <https://doi.org/10.1007/s00382-020-05333-z>.
- Bédard, J., Laroche, S. and Gauthier, P. (2015) A geo-statistical observation operator for the assimilation of near-surface wind data. *Quarterly Journal of the Royal Meteorological Society*, 141(692), 2857–2868. <https://doi.org/10.1002/qj.2569>.
- Blender, R., Raible, C. and Franzke, C. (2017) Vorticity and geopotential height extreme values in ERA-interim data during boreal winters. *Quarterly Journal of the Royal Meteorological Society*, 143(703), 634–640. <https://doi.org/10.1002/qj.2944>.
- Bojinski, S., Verstraete, M., Peterson, T.C., Richter, C., Simmons, A. and Zemp, M. (2014) The concept of essential climate variables in support of climate research, applications, and policy. *Bulletin of the American Meteorological Society*, 95(9), 1431–1443. <https://doi.org/10.1175/BAMS-D-13-00047.1>.
- Bollmeyer, C., Keller, J.D., Ohlwein, C., Wahl, S., Crewell, S., Friederichs, P., Hense, A., Keune, J., Kneifel, S., Pscheidt, I., Redl, S. and Steinke, S. (2015) Towards a high resolution regional reanalysis for the European CORDEX domain. *Quarterly Journal of the Royal Meteorological Society*, 141(686), 1–15. <https://doi.org/10.1002/qj.2486>.
- Bromwich, D.H., Wilson, A.B., Bai, L., Moore, G.W.K. and Bauer, P. (2016) A comparison of the regional Arctic system reanalysis and the global ERA-interim reanalysis for the Arctic. *Quarterly Journal of the Royal Meteorological Society*, 142, 644–658. <https://doi.org/10.1002/qj.2527>.
- Bromwich, D., Kuo, Y.-H., Serreze, M., Walsh, J., Bai, L.S., Barlage, M., Hines, K. and Slater, A. (2011) Arctic system reanalysis: call for community involvement. *Eos, Transactions, American Geophysical Union*, 91, 13–14. <https://doi.org/10.1029/2010EO020001>.
- Dahlgren, P., Landelius, T., Källberg, P. and Golvik, S. (2016) A high-resolution regional reanalysis for Europe. Part 1: Three-dimensional reanalysis with the regional High-resolution limited-area model (HIRLAM). *Quarterly Journal of the Royal Meteorological Society*, 142(698), 2119–2131. <https://doi.org/10.1002/qj.2807>.
- Dee, D.P., Uppala, S.M., Simmons, A.J., Berrisford, P., Poli, P., Kobayashi, S., Andrae, U., Balmaseda, M.A., Balsamo, G., Bauer, P., Bechtold, P., Beljaars, A.C.M., Van de Berg, L., Bidlot, J., Bormann, N., Delsol, C., Dragani, R., Fuentes, M., Geer, A.J., Haimberger, L., Healy, S.B., Hersbach, H., Hölm, E. V., Isaksen, L., Källberg, P., Köhler, M., Matricardi, M., McNally, A.P., Monge-Sanz, B.M., Morcrette, J.J., Park, B.K., Peubey, C., De Rosnay, P., Tavolato, C., Thépaut, J.N. and Vitart, F. (2011) The ERA-interim reanalysis: configuration and performance of the data assimilation system. *Quarterly Journal of the Royal Meteorological Society*, 137(656), 553–597. <https://doi.org/10.1002/qj.828>.
- Ding, Y., Shi, X., Liu, Y., Liu, Y., Li, Q., Qian, Y., Miao, M., Zhai, G. and Gao, K. (2006) Multi-year simulations and experimental seasonal predictions for rainy seasons in China by using a nested regional climate model (RegCM_NCC). Part I: Sensitivity study. *Advances in Atmospheric Sciences*, 23(3), 323–341. <https://doi.org/10.1007/s00376-006-0323-8>.
- Dulière, V., Zhang, Y. and Salathé, E.P., Jr. (2011) Extreme precipitation and temperature over the US Pacific northwest: A comparison between observations, reanalysis data, and regional models. *Journal of Climate*, 24(7), 1950–1964. <https://doi.org/10.1175/2010JCLI3224.1>.
- Gao, X., Xu, Y., Zhao, Z., Pal, J.S. and Giorgi, F. (2006) Impacts of horizontal resolution and topography on the numerical simulation of east Asian precipitation. *Chinese Journal of Atmospheric Sciences*, 30(2), 185.
- Gui, S., Yang, R., Cao, J. and Huang, W. (2020) Precipitation over East Asia simulated by ECHAM6. 3 with different schemes of cumulus convective parameterization. *Climate Dynamics*,

- 54(9–10), 4233–4261. <https://doi.org/10.1007/s00382-020-05226-1>.
- He, J., Zhang, F., Chen, X., Bao, X., Chen, D., Kim, H.M., Lai, H.W., Leung, L.R., Ma, X., Meng, Z., Ou, T., Xiao, Z., Yang, E.G. and Yang, K. (2019) Development and evaluation of an ensemble-based data assimilation system for regional reanalysis over the Tibetan plateau and surrounding regions. *Journal of Advances in Modeling Earth Systems*, 11(8), 2503–2522. <https://doi.org/10.1029/2019MS001665>.
- Hersbach, H., Bell, B., Berrisford, P., Hirahara, S., Horányi, A., Muñoz-Sabater, J., Nicolas, J., Peubey, C., Radu, R., Schepers, D., Simmons, A., Soci, C., Abdalla, S., Abellán, X., Balsamo, G., Bechtold, P., Biavati, G., Bidlot, J., Bonavita, M., Chiara, G., Dahlgren, P., Dee, D., Diamantakis, M., Dragani, R., Flemming, J., Forbes, R., Fuentes, M., Geer, A., Haimberger, L., Healy, S., Hogan, R.J., Hólm, E., Janisková, M., Keeley, S., Laloyaux, P., Lopez, P., Lupu, C., Radnoti, G., Rosnay, P., Rozum, I., Vamborg, F., Villaume, S. and Thépaut, J.N. (2020) The ERA5 global reanalysis. *Quarterly Journal of the Royal Meteorological Society*, 146(730), 1999–2049. <https://doi.org/10.1002/qj.3803>.
- Hong, S.Y., Noh, Y. and Dudhia, J. (2006) A new vertical diffusion package with an explicit treatment of entrainment processes. *Monthly Weather Review*, 134, 2318–2341. <https://doi.org/10.1175/MWR3199.1>.
- Hu, Z., Hu, Q., Zhang, C., Chen, X. and Li, Q. (2016) Evaluation of reanalysis, spatially-interpolated and satellite remotely-sensed precipitation datasets in Central Asia: Central Asia precipitation. *Journal of Geophysical Research*, 121, 5648–5663. <https://doi.org/10.1002/2016JD024781>.
- Huang, W.R., Chan, J.C.L. and Au-Yeung, A.Y.M. (2013) Regional climate simulations of summer diurnal rainfall variations over East Asia and Southeast China. *Climate Dynamics*, 40(7–8), 1625–1642. <https://doi.org/10.1007/s00382-012-1457-2>.
- Huffman, G.J., Bolvin, D.T., Nelkin, E.J., Wolff, D.B., Adler, R.F., Gu, G., Hong, Y., Bowman, K.P. and Stocker, E.F. (2007) The TRMM multisatellite precipitation analysis (TMPA): quasi-global, multiyear, combined-sensor precipitation estimates at fine scales. *Journal of Hydrometeorology*, 8(1), 38–55. <https://doi.org/10.1175/JHM560.1>.
- Hwang, S., Cho, J. and Yoon, K.S. (2018) Assessing the skills of CMIP5 GCMs in reproducing spatial climatology of precipitation over the coastal area in East Asia. *Journal of Korea Water Resources Association*, 51(8), 629–642. <https://doi.org/10.3741/JKWRA.2018.51.8.629>.
- Iacono, M.J., Delamere, J.S., Mlawer, E.J., Shephard, M.W., Clough, S.A. and Collins, W.D. (2008) Radiative forcing by long-lived greenhouse gases: calculations with the AER radiative transfer models. *Journal of Geophysical Research*, 113, D13103. <https://doi.org/10.1029/2008JD009944>.
- Janjic, Z.I. (1994) The step-mountain eta coordinate model: further developments of the convection, viscous sublayer and turbulence closure schemes. *Monthly Weather Review*, 122, 927–945. [https://doi.org/10.1175/1520-0493\(1994\)122<0927:TSMECM>2.0.CO;2](https://doi.org/10.1175/1520-0493(1994)122<0927:TSMECM>2.0.CO;2).
- Jiang, H., Yang, Y., Wang, H., Bai, Y. and Bai, Y. (2020) Surface diffuse solar radiation determined by reanalysis and satellite over East Asia: evaluation and comparison. *Remote Sensing*, 12(9), 1387. <https://doi.org/10.3390/rs12091387>.
- Joyce, R.J., Janowiak, J.E., Arkin, P.A. and Xie, P. (2004) CMORPH: A method that produces global precipitation estimates from passive microwave and infrared data at high spatial and temporal resolution. *Journal of Hydrometeorology*, 5(3), 487–503. [https://doi.org/10.1175/1525-7541\(2004\)005<0487:CAMTPG>2.0.CO;2](https://doi.org/10.1175/1525-7541(2004)005<0487:CAMTPG>2.0.CO;2).
- Kain, J.S. (2004) The Kain–Fritsch convective parameterization: an update. *Journal of Applied Meteorology*, 43, 170–181. [https://doi.org/10.1175/1520-0450\(2004\)043<0170:TKCPAU>2.0.CO;2](https://doi.org/10.1175/1520-0450(2004)043<0170:TKCPAU>2.0.CO;2).
- Kang, I.S., Jin, K., Wang, B., Lau, K.-M., Shukla, J., Krishnamurthy, V., Schubert, S., Wailser, D., Stern, W., Kitoh, A., Meehl, G., Kanamitsu, M., Galin, V., Satyan, V., Park, C.-K. and Liu, Y. (2002) Intercomparison of the climatological variations of Asian summer monsoon precipitation simulated by 10 GCMs. *Climate Dynamics*, 19(5–6), 383–395. <https://doi.org/10.1007/s00382-002-0245-9>.
- Kobayashi, S., Ota, Y., Harada, Y., Ebita, A., Moriya, M., Onoda, H., Onogi, K., Kamahori, H., Kobayashi, C., Endo, H., Miyaoka, K. and Takahashi, K. (2015) The JRA-55 reanalysis: general specifications and basic characteristics. *Journal of the Meteorological Society of Japan. Series II*, 93(1), 5–48. <https://doi.org/10.2151/jmsj.2015-001>.
- Lei, Y., Letu, H., Shang, H. and Shi, J. (2020) Cloud cover over the Tibetan plateau and eastern China: a comparison of ERA5 and ERA-interim with satellite observations. *Climate Dynamics*, 54(5–6), 2941–2957. <https://doi.org/10.1007/s00382-020-05149-x>.
- Li, Y.P., Wang, D.H. and Yin, J. (2018) Evaluations of different boundary layer schemes on low-level wind prediction in western Inner Mongolia. *Acta Scientiarum Naturalium Universitatis Sunyatseni*, 59(4), 16–29. <https://doi.org/10.13471/j.cnki.actasnu.2018.04.003>.
- Mesinger, F., DiMego, G., Kalnay, E., Mitchell, K., Shafran, P.C., Ebisuzaki, W., Jović, D., Woollen, J., Rogers, E., Berbery, E.H., Ek, M.B., Fan, Y., Grumbine, R., Higgins, W., Li, H., Lin, Y., Manikin, G., Parrish, D. and Shi, W. (2006) North American regional reanalysis. *Bulletin of the American Meteorological Society*, 87(3), 343–360. <https://doi.org/10.1175/BAMS-87-3-343>.
- Moore, G.W.K. and Renfrew, I.A. (2014) A new look at Southeast Greenland barrier winds and katabatic flow. *US CLIVAR Variations Newsletter*, 12(2), 1–19.
- Niu, G.X., Yang, Z.L., Mitchell, K.E., Chen, F., Michael, B.E., Barlage, M., Kumar, A., Manning, K., Niyogi, D., Rosero, E., Tewari, M. and Xia, Y. (2011) The community Noah land surface model with multiparameterization options (Noah-MP): 1. Model description and evaluation with local-scale measurements. *Journal of Geophysical Research*, 116, D12109. <https://doi.org/10.1029/2010JD015139>.
- Pu, Z. (2017) *Surface Data Assimilation and Near-Surface Weather Prediction Over Complex Terrain//Data Assimilation for Atmospheric, Oceanic and Hydrologic Applications (Vol. III)*. Cham: Springer, pp. 219–240.
- Quinting, J.F. and Vitart, F. (2019) Representation of synoptic-scale Rossby wave packets and blocking in the S2S prediction project database. *Geophysical Research Letters*, 46(2), 1070–1078. <https://doi.org/10.1029/2018GL081381>.
- Rood, R.B. and Bosilovich, M.G. (2010) *Reanalysis: Data Assimilation for Scientific Investigation of Climate//Data Assimilation*. Berlin, Heidelberg: Springer, pp. 623–646.

- Saha, S., Moorthi, S., Pan, H.L., Wu, X., Wang, J., Nadiga, S., Tripp, P., Kistler, R., Woollen, J., Behringer, D., Liu, H., Stokes, D., Grumbine, R., Gayno, G., Wang, J., Hou, Y.T., Chuang, H.Y., Juang, H.M.H., Sela, J., Iredell, M., Treadon, R., Kleist, D., Van Delst, P., Keyser, D., Derber, J., Ek, M., Meng, J., Wei, H., Yang, R., Lord, S., Van den Dool, H., Kumar, A., Wang, W., Long, C., Chelliah, M., Xue, Y., Huang, B., Schemm, J.K., Ebisuzaki, W., Lin, R., Xie, P., Chen, M., Zhou, S., Higgins, W., Zou, C.Z., Liu, Q., Chen, Y., Han, Y., Cucurull, L., Reynolds, R.W., Rutledge, G. and Goldberg, M. (2010) The NCEP climate forecast system reanalysis. *Bulletin of the American Meteorological Society*, 91(8), 1015–1058. <https://doi.org/10.1175/2010BAMS3001.1>.
- Skamarock, W.C., Klemp, J.B., Dudhia, J., Gill, D.O., Barker, D.M. and Powers, J.G. (2008) *A Description of the Advanced Research WRF Version 3 (No. NCAR/TN-475+STR)*. Boulder, CO: University Corporation for Atmospheric Research.
- Su, C.H., Eizenberg, N., Steinle, P., Jakob, D., Fox-Hughes, P., White, C.J., Rennie, S., Franklin, C., Dharssi, I. and Zhu, H. (2019) BARRA v1. 0: the Bureau of Meteorology atmospheric high-resolution regional reanalysis for Australia. *Geoscientific Model Development*, 12(5), 2049–2068. <https://doi.org/10.5194/gmd-12-2049-2019>.
- Sun, Q., Miao, C., Duan, Q., Ashouri, H., Sorooshian, S. and Hsu, K.-L. (2018) A review of global precipitation data sets: data sources, estimation, and intercomparisons. *Reviews of Geophysics*, 56(1), 79–107.
- Taylor, K.E. (2001) Summarizing multiple aspects of model performance in a single diagram. *Journal of Geophysical Research: Atmospheres*, 106(D7), 7183–7192. <https://doi.org/10.1029/2000JD900719>.
- Thompson, G., Paul, R.F., Roy, M.R. and William, D.H. (2008) Explicit forecasts of winter precipitation using an improved bulk microphysics scheme. Part II: implementation of a new snow parameterization. *Monthly Weather Review*, 136, 5095–5115. <https://doi.org/10.1175/2008MWR2387.1>.
- Wahl, S., Bollmeyer, C., Crewell, S., Figura, C., Friederichs, P., Hense, A., Keller, J.D. and Ohlwein, C. (2017) A novel convective-scale regional reanalysis COSMO-REA2: improving the representation of precipitation. *Meteorologische Zeitschrift*, 26(4), 345–361. <https://doi.org/10.1127/metz/2017/0824>.
- Whelan, E., Gleeson, E. and Hanley, J. (2018) An evaluation of MERA, a high-resolution mesoscale regional reanalysis. *Journal of Applied Meteorology and Climatology*, 57(9), 2179–2196. <https://doi.org/10.1175/JAMC-D-17-0354.1>.
- Wu, J. and Gao, X.J. (2013) A gridded daily observation dataset over China region and comparison with the other datasets. *Chinese Journal of Geophysics*, 56(4), 1102–1111 (in Chinese). <https://doi.org/10.6038/cjg20130406>.
- Wu, J., Gao, X.J., Giorgi, F. and Chen, D.L. (2017) Changes of effective temperature and cold/hot days in late decades over China based on a high resolution gridded observation dataset. *International Journal of Climatology*, 37, 788–800. <https://doi.org/10.1002/joc.5038>.
- Xu, J., Rugg, S., Byerle, L. and Liu, Z. (2009) Weather forecasts by the WRF-ARW model with the GSI data assimilation system in the complex terrain areas of Southwest Asia. *Weather and Forecasting*, 24(4), 987–1008. <https://doi.org/10.1175/2009WAF222229.1>.
- Yang, E.G. and Kim, H.M. (2017) Evaluation of a regional reanalysis and ERA-interim over East Asia using in situ observations during 2013–14. *Journal of Applied Meteorology and Climatology*, 56(10), 2821–2844. <https://doi.org/10.1175/JAMC-D-16-0227.1>.
- Yang, L., Wang, S., Tang, J., Niu, X. and Fu, C. (2019) Evaluation of the effects of a multiphysics ensemble on the simulation of an extremely hot summer in 2003 over the CORDEX-EA-II region. *International Journal of Climatology*, 39, 3413–3430. <https://doi.org/10.1002/joc.6028>.
- Yang, Y., Wang, Y. and Zhu, K. (2015) Assimilation of Chinese doppler radar and lightning data using WRF-GSI: a case study of mesoscale convective system. *Advances in Meteorology*, 2015, 1–17. <https://doi.org/10.1155/2015/763919>.
- Yao, B., Liu, C., Yin, Y., Liu, Z., Shi, C., Iwabuchi, H. and Weng, F. (2020) Evaluation of cloud properties from reanalyses over East Asia with a radiance-based approach. *Atmospheric Measurement Techniques*, 13(3), 1033–1049. <https://doi.org/10.5194/amt-13-1033-2020>.
- Yin, J., Wang, D. and Zhai, G. (2014) A study of characteristics of the cloud microphysical parameterization schemes in meso-scale models and its applicability to China. *Advances in Earth Science*, 29(2), 238–249.
- Yin, J.F., Liang, X.D., Chen, F., Liu, Y., He, H.Z., Liang, Z.M., Zou, H.B., Xu, J.J., Hao, S.F. and XIE, Y.X. (2018) Development of atmospheric data assimilation techniques and regional reanalysis datasets in the East Asia. *Advances in Meteorological Science and Technology*, 8(1), 79–84.
- Zakeri, Z., Azadi, M. and Ghader, S. (2018) The impact of different background errors in the assimilation of satellite radiances and in-situ observational data using WRFDA for three rainfall events over Iran. *Advances in Space Research*, 61(1), 433–447. <https://doi.org/10.1016/j.asr.2017.10.011>.
- Zhang, Q., Pan, Y., Wang, S., Xu, J. and Tang, J. (2017) High-resolution regional reanalysis in China: evaluation of 1 year period experiments. *Journal of Geophysical Research: Atmospheres*, 122(20), 10801–10819. <https://doi.org/10.1002/2017JD027476>.
- Zhu, Y.Y. and Yang, S. (2020) Evaluation of CMIP6 for historical temperature and precipitation over the Tibetan plateau and its comparison with CMIP5. *Advances in Climate Change Research*, 11(3), 239–251. <https://doi.org/10.1016/j.accre.2020.08.001>.

How to cite this article: Yang, L., Liang, X., Yin, J., Xie, Y., & Fan, H. (2023). Evaluation of the precipitation of the East Asia regional reanalysis system mainly over mainland China. *International Journal of Climatology*, 43(4), 1676–1692. <https://doi.org/10.1002/joc.7940>